Intrinsic impaired proplatelet formation and microtubule coil assembly of megakaryocytes in a mouse model of Bernard-Soulier syndrome

Catherine Strassel, Anita Eckly, Catherine Léon, Claire Petitjean, Monique Freund, Jean-Pierre Cazenave, Christian Gachet, and François Lanza

UMR-S949 INSERM, Université de Strasbourg, EFS-Alsace, Strasbourg, France

ABSTRACT

Background

Giant platelets and thrombocytopenia are invariable defects in the Bernard-Soulier syndrome caused by deficiency of the GPIb-V-IX complex, a receptor for von Willebrand factor supporting platelet adhesion to the damaged arterial wall. Various properties of this receptor may be considered potential determinants of the macrothrombocytopenia.

Design and Methods

To explore the underlying mechanisms of the disease, megakaryopoiesis was studied in a mouse model deficient in GPIbβ. Megakaryocytes were initially characterized *in situ* in the bone marrow of adult mice, after which their capacity to differentiate into proplatelet-bearing cells was evaluated in cultured fetal liver cells.

Results

The number of megakaryocyte progenitors, their differentiation and progressive maturation into distinct classes and their level of endoreplication were normal in GPIbβ$^{-/-}$ bone marrow. However, the more mature cells exhibited ultrastructural anomalies with a thicker peripheral zone and a less well developed demarcation membrane system. GPIbβ$^{-/-}$ megakaryocytes could be differentiated in culture from Lin^{-} fetal liver cells in normal amounts but the proportion of cells able to extend proplatelets was decreased by 41%. Moreover, the GPIbβ$^{-/-}$ cells extending proplatelets displayed an abnormal morphology characterized by fewer pseudopodial extensions with thicker shaft sections and an increased diameter of the terminal coiled elements. GPIbβ$^{-/-}$ released platelets were larger but retained a typical discoid shape. Proplatelet formation was similarly affected in bone marrow explants from adult mice examined by videomicroscopy. The marginal microtubular ring contained twice as many tubulin fibers in GPIbβ$^{-/-}$ proplatelet buds in cultured and circulating platelets.

Conclusions

Altogether, these findings point to a role of the GPIb-V-IX complex intrinsic to megakaryocytes at the stage of proplatelet formation and suggest a functional link with the underlying microtubular cytoskeleton in platelet biogenesis.

Key words: megakaryocyte, platelet, Bernar-Soulier, microtubules, GPIb-V-IX.

Citation: Strassel C, Eckly A, Léon C, Petitjean C, Freund M, Cazenave J-P, Gachet C, and Lanza F. Intrinsic impaired proplatelet formation and microtubule coil assembly of megakaryocytes in a mouse model of Bernard-Soulier syndrome. Haematologica 2009; 94:800-810. doi:10.3324/haematol.2008.001032

Acknowledgments: we thank M Souyri for helpful discussions, JY Rinckel, F Proamer and S Moog for expert technical assistance and JN Mulvihill for reviewing the English of the manuscript.

Manuscript received September 23, 2008. Revised version arrived January 16, 2009. Manuscript accepted January 16, 2009.

Correspondence: François Lanza, INSERM U949, EFS-Alsace, 10 rue Spielmann 67000 Strasbourg. E-mail: francois.lanza@efs-alsace.fr

The online version of this article contains a supplementary appendix.

Introduction

Hereditary deficiency of the platelet GPIb-V-IX complex leads to a rare bleeding disorder first reported in 1948 by Jean Bernard and Jean-Pierre Soulier.[1] This disease was named *dystrophie thrombocytaire hémorragipare* in view of the presence of greatly enlarged platelets (dystrophic thrombocytes) in blood smears. The morphological alterations of platelets and associated thrombocytopenia are still poorly understood features of this disorder now commonly designated as Bernard-Soulier syndrome. Following the seminal observation, deficiency of the glycoprotein (GP) Ib-V-IX complex was established as the molecular cause of the disease.[2] This led to the identification of GPIb-V-IX as a receptor for von Willebrand factor supporting platelet adhesion to the damaged arterial wall.[3] In contrast, little information is available concerning the role of GPIb-V-IX in platelet biogenesis and how its deficiency induces macrothrombocytopenia.[4,5]

The prevailing hypothesis is that the abnormal platelet size and decreased platelet count stem from defective megakaryopoiesis, although a shortened platelet half-life could also contribute to the thrombocytopenia.[6] Due to the rarity of the disease and the bleeding risk associated with marrow biopsies, megakaryocytes from Bernard-Soulier patients have only rarely been examined.[6-8] Tomer *et al*. reported a normal proportion of identifiable megakaryocytes in bone marrow smears, with a slight increase in cell size and an increased ploidy.[6] Hourdillé *et al*. observed a normal cell size but an abnormal demarcation membrane system with a vacuolar appearance.[7] More recently, analysis of bone marrow from mice lacking the GPIbα subunit revealed an underdeveloped demarcation membrane system.[9] Altogether, these studies suggest that the GPIb-V-IX complex could play a role in the late stages of megakaryopoiesis, at times coinciding with the expression of the receptor.[10,11]

Various properties of the receptor may be considered to be potential determinants of macrothrombocytopenia, including its extracellular ligand binding, intracellular signaling and membrane structuring properties.[12] Macrothrombocytopenia has not been reported in patients or mice deficient in three known GPIb-V-IX ligands, von Willebrand factor, P-selectin and integrin $\alpha_M\beta_2$, which would argue against the involvement of the extracellular binding domain.[13,14] On the other hand, impaired megakaryopoiesis has been observed in a thrombocytopenic patient with a mutation in the GPIbα interacting site of von Willebrand factor,[15] while decreased megakaryocyte differentiation has been observed in $CD34^+$ cells cultured in the presence of antibodies against the extracellular portion of GPIbα.[16] The intracellular properties of the receptor have also been incriminated in defective platelet biogenesis in relation to the linkage of GPIb-V-IX to the submembranous actin cytoskeleton, which is mediated by filamin.[17] Actin reorganization, with the participation of PKCα, appears to be important for the formation of proplatelet extensions, but the involvement of a GPIb-actin link in this process has not been established.[18,19] Finally, as GPIb-V-IX is expressed at high density on the cell surface (24,000 copies/platelet), it could represent a membrane structuring element in the course of proplatelet formation.

Although the available studies of GPIb-V-IX-deficient megakaryocytes provide interesting morphological and ultrastructural images of the native tissue, they do not inform about the dynamic process leading to platelet biogenesis.[9,20] Megakaryocyte progenitors can now be cultured efficiently and these techniques can be applied to mouse strains with selected deficiencies, allowing examination of the entire process leading to platelet production.[21,22] The final step in this process is typified by the extension of numerous proplatelets from the surface of mature megakaryocytes, in the form of long pseudopodia bearing organized platelet elements at their extremities.[23] This requires the recruitment of an internal pool of membranes[24] and dynamic reorganization of the microtubules, which drive the extension of pseudopodia and coil up to delimit disc-shaped platelet elements.[25] The recent live visualization of fluorescent-labeled megakaryocytes in transgenic mice has added support for this model, showing proplatelet elements protruding into bone marrow sinusoids.[26]

In an attempt to analyze the role played by GPIb-V-IX in megakaryopoiesis and identify the abnormal mechanisms occurring in its absence, we studied mice lacking the GPIbβ subunit which recapitulate the Bernard-Soulier syndrome, including the associated macrothrombocytopenia.[27] Megakaryocytes were initially characterized *in situ* in the bone marrow of adult mice, after which their capacity to differentiate into proplatelet-bearing cells was evaluated in cultured fetal liver cells.

Design and Methods

Animals

Mice lacking expression of the GPIbβ subunit ($GPIb\beta^{-/-}$) in which the coding sequence of GPIbβ has been replaced by a neo cassette have been described previously.[27] These mice were backcrossed for seven generations on a C57Bl/6 background and maintained in the animal facilities of the Etablissement Français du Sang-Alsace, Strasbourg, France. Ethical approval for animal experiments was received from the French Ministry of Research in accordance with European Union guidelines.

Bernard-Soulier syndrome patients

Unrelated patients (BSS.1, BSS.2) were 30- and 24-year old French women found to have macrothrombocytopenia in routine blood examinations. They were diagnosed as having classic Bernard-Soulier syndrome following the discovery of absent ristocetin-induced agglutination and profound decreases in the platelet GPIb-V-IX complex as revealed by flow cytometry using the Cytoquant assay (Biocytex, Marseille, France).

Kinetics of platelet survival

The platelet survival time was determined by *in vivo* biotinylation of platelets by intravenous injection of sulpho-NHS-LC-biotin (2 mg/kg twice at a 30 min inter-

val, five mice of each genotype).[28] The percentage of biotinylated platelets was determined for 4 days at 7 h intervals by flow cytometric analysis of whole blood samples double labeled with streptavidin-phycoerythrin (100 μg/mL) and anti-CD41/CD61-phycoerythrin. Platelet survival was estimated from the decay curve of the proportion of biotinylated platelets over time.

Bone marrow histology

Bone marrow was harvested by flushing mouse femora with Hank's buffered salt solution (HBSS) at physiological pH and osmolarity. The samples were immediately fixed for 24 h in 4% paraformaldehyde and embedded in paraffin, or in OCT tissue freezing medium (OCT Tissue-Tek®, EMS, Hatfield, USA) to prepare cryosections. Sections with a thickness of 5 μm were cut. Paraffin-embedded sections were stained with hematoxylin and eosin (H&E). Cryosections were stained with phalloidin-TRITC (100 ng/mL; Sigma-Aldrich, St. Louis, MO, USA) and a rat monoclonal antibody (LucA5) against mouse GPIIb-IIIa (CD41) (EMFRET, Würzburg, Germany) conjugated with Alexa-488 (Jackson Immunoresearch, West Grove, PA, USA). Samples were examined under a confocal microscope (TCS SP5, objective 63X/1.4 oil, Leica Microsystems, France).

Hematopoietic progenitor cell assays

Single cell suspensions of bone marrow (1.5×10^4 cells/mL) were cultured in 1.2 mL of MethoCult M3434 (Stem Cell Technologies, Vancouver, Canada) supplemented with 50 ng/mL recombinant human thrombopoietin (rhTPO, Stem Cell Technologies). Colony-forming units (CFU-GM), burst-forming units (BFU-E), CFU-Mk and CFU-GEMM were identified by their morphology and counted under an inverted microscope 7 days after plating (eight independent experiments were performed for each strain).

Megakaryocyte cultures

Livers were recovered from mouse fetuses between embryonic days 13 and 15. After Lin-selection (Stem Cell Technologies), single cell suspensions were cultured for 4 days in Dulbecco's modified Eagle's medium (DMEM) supplemented with 10% fetal bovine serum (Stem Cell Technologies), 2 mmol/L L-glutamine, 50 U/mL penicillin, 50 μg/mL streptomycin and 50 ng/mL rhTPO.

Bone marrow explants time-lapse analysis

Bone marrows from GPIbβ$^{+/+}$ or GPIbβ$^{-/-}$ mice were obtained by flushing femora with Tyrode's buffer. The marrows were cut in transverse sections of 0.5 mm and placed in an incubation chamber containing Tyrode's buffer supplemented with 5% mouse serum. Each chamber contained 12 fragments and was maintained at 37°C for 6 h. Megakaryocytes at the periphery of the tissue were observed under a phase contrast microscope (Leica DMIRB, Leica Microsystems SA, Westlar, Germany) (63x objective) coupled to a video camera (DAGE MTI, Michigan City, MI, USA). Images were acquired sequentially at 5 second intervals and processed with Metamorph™ software (Universal Imaging Corporation, Downingtown, PA, USA). Cells were classified according to their morphology as round shaped, megakaryocytes with membrane protusions and megakaryocytes with proplatelets. Three mice with each genotype were analyzed.

DNA content of megakaryocytes

Bone marrow suspensions were prepared in phosphate-buffered saline (PBS)-citrate-bovine serum albumin (BSA) buffer (PBS containing 0.38% sodium citrate and 0.5% BSA) in plastic tubes. Cells ($1\text{-}5\times10^6$) were labeled for 30 min at 4°C with 1.25 μg of a fluorescein isothiocyanate (FITC)-conjugated monoclonal antibody against CD41 (rat anti-mouse glycoprotein IIb; Pharmingen, San Diego, CA, USA) and gently washed twice in PBS-citrate. The pellet was resuspended in 200 μL of PBS and 4 mL of a cold solution of 70% ethanol in PBS was added. After incubation for 1 h at 4°C, the suspension was centrifuged, the cells were resuspended in 100 μL of PBS and propidium iodide (2 mL [50 μg/mL]) and RNAase (100 μg/mL) in PBS were added for 30 min at 37°C. The ploidy distribution in the CD41$^+$ population was determined by two-color flow cytometry (FACScalibur; Becton Dickinson, San José, CA, USA).

Immunofluorescence microscopy

Cultured megakaryocytes were cytocentrifuged onto poly L-lysine-coated coverslips, fixed in 2% paraformaldehyde (PFA) for 15 min, washed and permeabilized with 0.05% saponin in PBS containing 0.2% BSA for 15 min. The cells were then incubated with a monoclonal antibody against β-tubulin (clone 2-28-33; Sigma-Aldrich) or RAM.2 against integrin αIIbβ3 (both 10 μg/mL) for 45 min in the same buffer, followed by secondary Cy3-conjugated goat anti-mouse or anti-rat antibodies, respectively. The coverslips were mounted in Mowiol for observation under a confocal microscope (TCS SP5, objective 63X/1.30 NA oil, Leica Microsystems) using LAS acquisition software (AF version 1.62; Leica).

Transmission electron microscopy

Washed platelets or bone marrow samples were fixed in 2.5% glutaraldehyde and embedded in epon. Thin sections were stained with uranyl acetate and lead citrate and examined under a CM120 transmission electron microscope (FEI, The Netherlands). Megakaryocytes at stages I, II and III were identified according to Zucker-Franklin using distinct ultrastuctural characteristics: stage I, a cell 10-50 μm in diameter with a large nucleus; stage II, a cell 20-80 μm in diameter containing platelet-specific granules; stage III, a megakaryocyte containing a well-developed demarcation membrane system (DMS) defining platelet territories and a peripheral zone (PZ). The DMS and PZ surface areas were measured in stage III cells using Methamorph™ software (Version 5; Universal Imaging Corporation, Downingtown, PA, USA). The DMS analysis was performed in GPIbβ$^{+/+}$ and GPIbβ$^{-/-}$ megakaryocytes (46

and 37 cells, respectively) by determining the area of the internal membrane systems in a region of interest (111±4 and 101±4 μm^2, respectively) of the cytoplasm. The PZ was quantified by measuring the surface area of the actin-rich external ring devoid of organelles and expressing it as the percentage of the total surface area (30 and 33 cells, respectively). Samples from three mice with each genotype were examined in each case.

To visualize the intracellular microtubules, bone marrow cells were permeabilized for 5 min with 0.02% saponin in PHEM (60 mM Pipes, 25 mM EGTA and 2 mM $MgCl_2$, pH 6.9) containing 5 μM phalloidin and 30 μM taxol, fixed in 2% PFA for 20 min and incubated overnight with a monoclonal antibody against β-tubulin (clone 2-28-33; Sigma-Aldrich) followed by 10 nm gold-conjugated protein A. The samples were then embedded in epon for transmission electron microscopy (TEM) as described above.

Scanning electron microscopy

To visualize the intracellular cytoskeletal filaments, cultured megakaryocytes were incubated for 5 min with 0.5% Triton X-100 in PHEM containing 0.1% glutaraldehyde, 5 μM phalloidin and 30 μM taxol. The resulting cytoskeletons were fixed in 1% glutaraldehyde for 10 min and allowed to adhere by sedimentation to the surface of poly-L-lysine-coated coverslips.[29] After three washes in PBS and dehydration in graded ethanol solutions, the samples were air-dried with hexamethyldisilazane, sputtered with gold and examined under a scanning electron microscope (Sirion, FEI, The Netherlands).

Megakaryocytes and platelet elements in culture suspensions were fixed in 2.5% glutaraldehyde and prepared for scanning electron microscopy as described above.

Platelet preparation

Washed platelets were prepared from ACD-anticoagulated blood by Ficoll separation from platelet-rich plasma and sequential centrifugation.[30] The cells were resuspended (3×10^5/μL) in Tyrode's buffer containing 0.35% human serum albumin and 0.02 U/mL potato apyrase.

Statistical analyses

Results were expressed as the mean (± SEM) and statistical analyses were performed using GraphPad Prism v3.00 for Windows (GraphPad Software, San Diego, CA, USA). Statistical differences were analyzed by non-parametric *t* tests. *p* values less than 0.05 were considered statistically significant.

Results

The platelet half-life is normal in GPIbβ$^{-/-}$ mice

To determine whether increased platelet consumption could be responsible for the thrombocytopenia observed in GPIbβ deficiency, platelet survival was monitored by flow cytometry after *in vivo* biotin labeling of platelets (Figure 1). The rate of disappearance of platelets from the circulation was not different in GPIbβ$^{-/-}$ and GPIbβ$^{+/+}$ mice, with estimated survival times of 3.8±0.1 and 4.2±0.1 days, respectively. This indicated that macrothrombocytopenia results from a defect during megakaryopoiesis.

GPIbβ$^{-/-}$ bone marrow contains normal numbers of megakaryocyte progenitors

To see whether the decreased platelet production was due to defective commitment of hematopoietic stem cells, bone marrow cells were analyzed in clonogenic assays in the presence of thrombopoietin. The numbers of colonies of megakaryocyte progenitors (CFU-Mk) scored in semisolid cultures were equivalent for GPIbβ$^{-/-}$ and GPIbβ$^{+/+}$ marrow (3±0.4 versus 3.9±0.7 colonies) (Figure 2A). Moreover, the numbers of other hematopoietic colonies (CFU-GM, BFU-E, CFU-E and CFU-GEMM) were also similar in the two strains. Hence the absence of the GPIb-V-IX complex did not impair stem cell commitment to the different lineages.

GPIbβ$^{-/-}$ bone marrow displays increased numbers of megakaryocytes but normal endoreplication

We next investigated whether GPIb-V-IX deficiency had an impact on megakaryocyte numbers or maturation. Numbers of mature bone marrow megakaryocytes, identified by their size on H&E-stained smears, were increased (147%) rather than decreased in GPIbβ$^{-/-}$ as compared to GPIbβ$^{+/+}$ marrow (Figures 2B,C). The thrombocytopenia was, therefore, not due to reduced numbers of megakaryocytes. The degree of polyploidy, a marker of megakaryocyte maturation, was assessed in bone marrow cells by measuring propidium iodide incorporation in the CD41$^+$ population gated by flow cytometry. The cell distribution in ploidy classes ranging from 2N to 32N was similar in GPIbβ$^{-/-}$and GPIbβ$^{+/+}$ megakaryocytes (Figure 2D), indicating that the absence of GPIb-V-IX did not affect endomitosis.

GPIbβ$^{-/-}$ bone marrow displays normal proportions of stage I-III megakaryocytes but ultrastructural defects of stage III cells

Megakaryocyte maturation was also examined ultrastructurally by TEM analysis of bone marrow aspirates. Megakaryocytes were ranked into three classes (stages

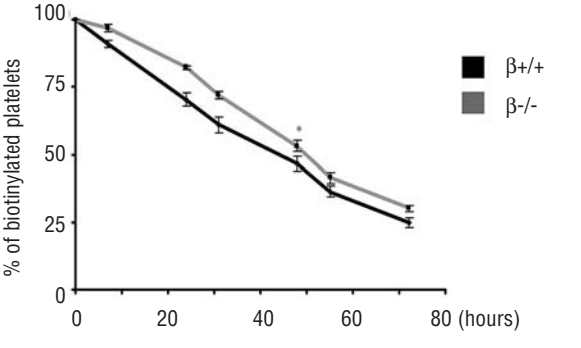

Figure 1. GPIbβ$^{-/-}$ platelets have a normal life span. Mice were injected i.v. with N-hydroxy-succinomidyl biotin on day 0 and the percentage of biotinylated platelets was determined at the indicated times using flow cytometry and CD41 gating. Data are the mean values±SEM of quadruple determinations.

I, II and III) on the basis of cell size, nuclear compactness, the presence of organelles and the development of platelet territories.[31] The distribution in the different maturation stages was not significantly different in GPIbβ$^{-/-}$ and GPIbβ$^{+/+}$ marrow (Figure 3A), indicating overall preservation of the maturation process in the absence of GPIb-V-IX. However, several ultrastructural anomalies were revealed in stage III GPIbβ$^{-/-}$ cells (Figure 3B). Greatly enlarged cytoplasmic territories and a concomitant underdeveloped DMS were observed, the latter representing half the GPIbβ$^{+/+}$ DMS surface area (9±0.6 *vs.* 21±1 μm^2 DMS/100μm^2, respec-

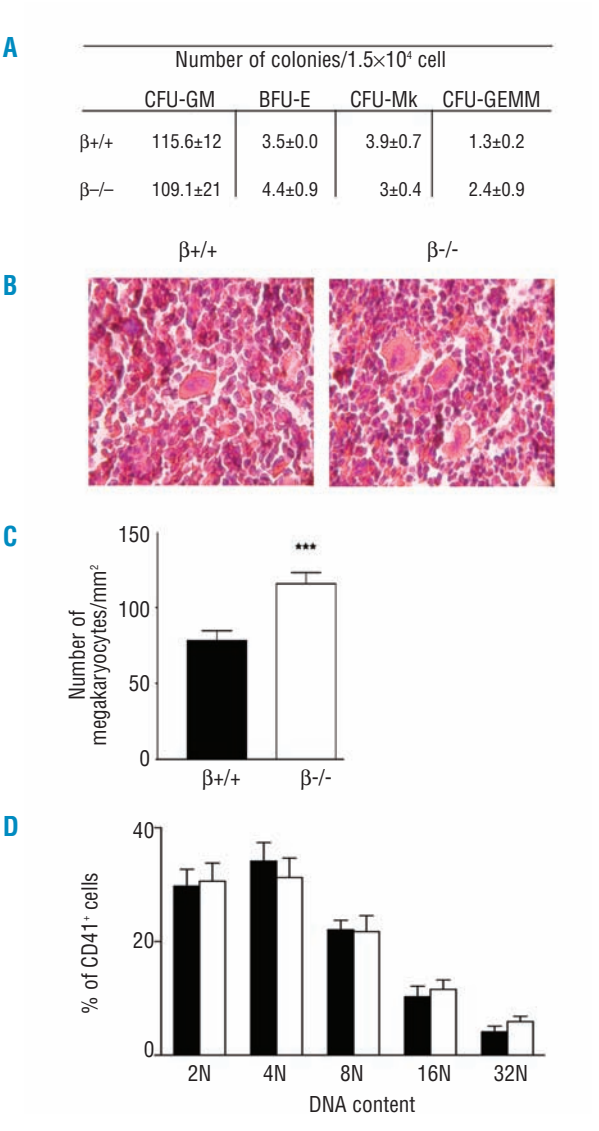

Figure 2. GPIbβ$^{-/-}$ bone marrow contains normal numbers of progenitors but increased numbers of identifiable megakaryocytes with a normal ploidy distribution. (A) Colony assays for CFU-Mk, CFU-GM, BFU-E and CFU-GEMM in bone marrow from GPIbβ$^{+/+}$ and GPIbβ$^{-/-}$ mice. Results are the mean±SEM of eight independent experiments and no significant differences were found between the two groups. (B) Representative sections of GPIbβ$^{+/+}$ and GPIbβ$^{-/-}$ mouse femora stained with H&E. (C) Morphologically recognizable megakaryocytes were counted and numbers expressed as the mean±SEM per mm^2 of surface in four or five fields from six mice in each group. Numbers of megakaryocytes were significantly increased in GPIbβ$^{-/-}$ mice, ***p<0.006. (D) Ploidy analysis of CD41$^+$ bone marrow cells from GPIbβ$^{+/+}$ and GPIbβ$^{-/-}$ mice. Data are the mean±SEM of four experiments with two mice per experiment in each group. The ploidy distribution was not significantly different in GPIbβ$^{+/+}$ and GPIbβ$^{-/-}$ cells.

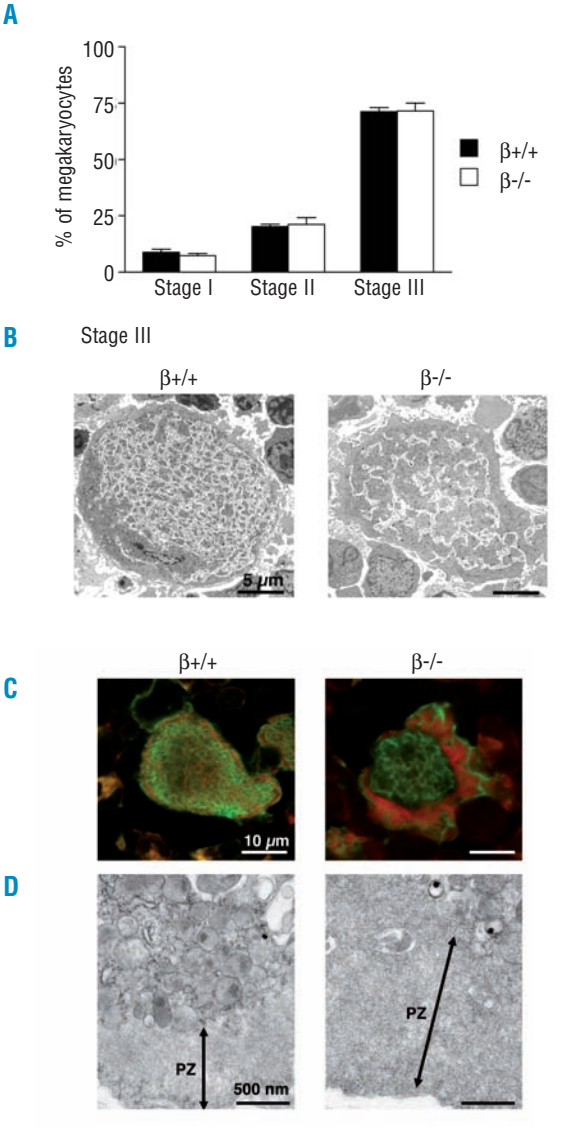

Figure 3. GPIbβ$^{-/-}$megakaryocytes display a normal distribution in different maturation stages but ultrastructural defects in stage III cells. (A) The distribution in the different maturation stages was established according to megakaryocyte morphology (see Methods) on TEM images and was not significantly different in GPIbβ$^{+/+}$ and GPIbβ$^{-/-}$ mice. Results are the mean±SEM of the percentage of megakaryocytes in each stage. (B) Representative TEM images of stage III megakaryocytes in the bone marrow of GPIbβ$^{+/+}$ and GPIbβ$^{-/-}$ mice. GPIbβ$^{-/-}$ cells display a poorly developed demarcation membrane system and increased size of the cytoplasmic platelet territories. (C) Representative confocal microscopic images of stage III megakaryocytes labeled with phalloidin-TRITC (red) and a monoclonal antibody against CD41 (green). GPIbβ$^{-/-}$ cells exhibit a wider actin-rich (red) and organelle-deficient peripheral zone (PZ) than GPIbβ$^{+/+}$ cells. (D) Detailed TEM images of the PZ in GPIbβ$^{+/+}$ and GPIbβ$^{-/-}$ megakaryocytes.

tively). In addition, the cells were delimited by a thicker peripheral zone, an area devoid of organelles, and enriched in cytoskeletal proteins (Figure 3C ,D).[32] This zone represented one third of the total cell surface area in GPIbβ$^{-/-}$ megakaryocytes (32.6±1.6%), almost double that in GPIbβ$^{+/+}$ cells (19.5±1.1%). Overall, *in situ* analysis pointed to defects in GPIbβ$^{-/-}$ megakaryocytes occurring late in thrombopoiesis in connection with the organization of membrane and cytoskeletal networks leading to the shedding of platelets.

Proplatelet formation is abnormal in GPIbβ$^{-/-}$ megakaryocytes differentiated from fetal liver cells

To identify the anomalies occurring during thrombopoiesis more precisely, fetal liver progenitors were differentiated in culture in the presence of thrombopoietin. After 4 days a majority of GPIbβ$^{+/+}$ cells had differentiated into CD41^{+} megakaryocytes exhibiting extensive fragmentation into numerous long and thin proplatelet extensions (Figure 4A). GPIbβ$^{-/-}$ progenitors also produced CD41^{+} megakaryocytes, but a significant proportion of the cells displayed a round morphology and failed to extend proplatelets. In six separate cultures, the frequency of proplatelet-bearing megakaryocytes was 31.8±2.9% in GPIbβ$^{-/-}$ and 54.8±3.3% in GPIbβ$^{+/+}$ cultures (Figure 4B). Defective proplatet formation was also observed at day 3 with a 1.9-fold decrease in proplatelet-bearing cells, whereas a similar low percentage of cells harbored proplatelets at day 2 (7.1±1.4% in GPIbβ$^{-/-}$ and 7.1±0.57% in GPIbβ$^{+/+}$ cultures). At day 1, all cells presented a round immature morphology in both strains (*data not shown*). Moreover, GPIbβ$^{-/-}$ progenitors which reached the proplatelet stage presented various abnormalities as compared to GPIbβ$^{-/-}$ cells (Figure 5A). The deficient cells exhibited a decreased degree of complexity with fewer pseudopodia, an increased size of the shaft sections (1157±74.3 *vs.* 440.7±20.5 nm) (Figure 5B) and a 2-fold increase in the diameter of the coiled elements (6.44±0.3 *vs.* 3.44±0.1 μm) (Figure 5B). Scanning electron microscopy showed the presence of free platelets in the culture suspensions (Figure 5C). However, the mean diameter was 30% greater in GPIbβ$^{-/-}$ as compared to GPIbβ$^{+/+}$ platelets (3.3±0.1 *vs.* 2.5±0.1 μm) (Figure 5D). This indicated that an intrinsic defect of thrombopoiesis was responsible for the enlarged platelet size in the GPIbβ$^{-/-}$ phenotype. Cultured and circulating GPIbβ$^{-/-}$ platelets nevertheless displayed a discoid shape, typical of the resting state in normal cells.

Proplatelet formation is abnormal in GPIbβ$^{-/-}$ megakaryocytes in bone marrow explants

To evaluate proplatelet formation in a more native microenvironment, adult mouse bone marrow samples were bathed in a physiological buffer and observed for 6 h by time-lapse microscopy. In GPIbβ$^{+/+}$, megakaryocytes were progressively observed at the explant periphery (Figure 6A). Over time, some cells retained a spherical shape, developed thick extensions, or extended numerous thin filopodia with extensive branching and decreased size of the cell body (Figure 6A, *Online Supplementary video*). In GPIbβ$^{-/-}$, the number of proplatelets was decreased and the proplatelet size was increased as compared to GPIbβ$^{+/+}$ (Figure 6B) and the number of megakaryocytes extending proplatelets was decreased by 2.8-fold (34.5±7.1 *vs.* 12±1.1 in GPIbβ$^{+/+}$) (Figure 6C). These results were very similar to those obtained from cultured cells.

Cultured and circulating GPIbβ$^{-/-}$ platelets contain increased numbers of microtubule coils

Since the maintenance of a discoid shape is dependent on the presence of an intact marginal microtubular ring, megakaryocytes differentiated in culture were examined for tubulin by immunofluorescence and electron microscopy. β-tubulin labeling of proplatelet-bearing cells was observed along the shaft sections and in the marginal band of the platelet buds, the thickness appearing to be greater in GPIbβ$^{-/-}$ than in GPIbβ$^{+/+}$ cells (Figure 5A). Scanning electron microscopy of permeabilized cells revealed thicker and less well organized bundles of microtubules in these two areas (Figure 7A). Consistent with these observations, TEM of platelets released into the culture medium showed a larger number of coils in the marginal band (Figure 7B). Similarly, immunogold labeling of β-tubulin in mature circulating platelets showed, on trans-

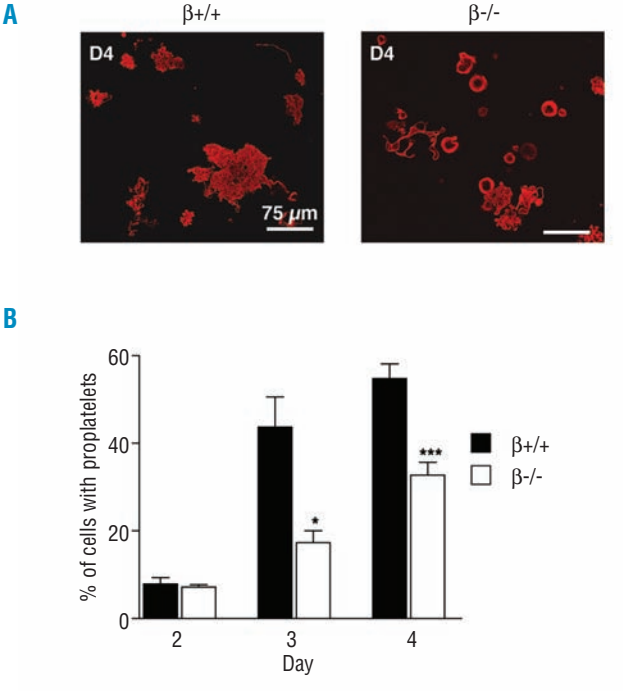

Figure 4. A decreased proportion of megakaryocytes extend proplatelets in cultures of GPIbβ$^{-/-}$ fetal liver cells. Lin^{-}selected fetal liver cells were cultured for 4 days in the presence of thrombopoietin and FBS and examined by confocal microscopy to determine the proportion of megakaryocytes bearing proplatelets. (A) Representative images of megakaryocytes stained for tubulin on day 4 showing a majority of proplatet-bearing GPIbβ$^{+/+}$ cells and an increased proportion of GPIbβ$^{-/-}$ cells with a round morphology which did not reach the proplatelet stage. (B) The number of CD41^{+} cells forming proplatelets was counted from day 2 to day 4 (no proplatelets were formed at day 1) and expressed as the percentage of the total number of CD41^{+} cells. A significant percentage extended proplatelets at days 3 and 4 in both strains. This proportion was decreased in GPIbβ$^{-/-}$, representing 31.8±2.9% versus 54.8±3.3% in GPIbβ$^{+/+}$ at day 4. Values are the mean±SEM of six separate experiments, ***p<0.001.

verse (Figure 7C) and cross sections (Figure 7D), a 2-fold increase in the mean number of microtubule rings per cell in GPIbβ$^{-/-}$ as compared to GPIbβ$^{+/+}$ platelets (22.2±1.8 *vs.* 11±0.6 turns) (Figure 7E).

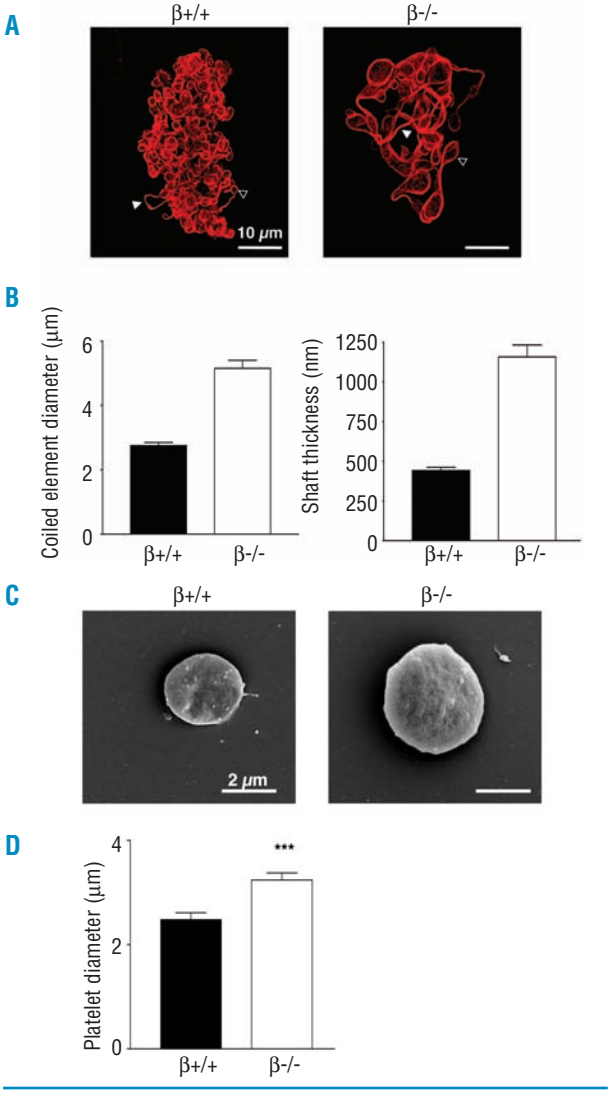

Figure 5. Proplatelet-bearing megakaryocytes and individual platelets have an abnormal morphology in cultures of GPIbβ$^{-/-}$ fetal liver cells. (A) Representative confocal photomicrographs of proplatelet-bearing megakaryocytes labeled for β-tubulin showing an extensive network with thin shafts (arrow) and platelet-sized coils (arrowhead) in GPIbβ$^{+/+}$ cells and a decreased number of proplatelet extensions, thicker shafts and enlarged coils in GPIbβ$^{-/-}$ cells. (B) The diameter of the coiled elements (in μm) and the shaft thickness (in nm) were measured on confocal photomicrographs using LAS acquisition software (AF version 1.62; Leica) and both parameters were increased in GPIbβ$^{-/-}$ as compared to GPIbβ$^{+/+}$ cells. Values are the mean±SEM of three separate experiments in each group. (C) Scanning electron microscopy images of platelets in the culture suspension show a characteristic discoid morphology and a smooth cell surface with openings corresponding to entrances to the open canalicular system. GPIbβ$^{-/-}$ platelets have a larger diameter than GPIbβ$^{+/+}$ cells but retain a disc-shaped morphology. (D) The mean diameter (±SEM) was measured on electron micrographs of 22 individual cultured platelets, ***p<0.001.

Discussion

The exact cause of macrothrombocytopenia in patients with Bernard-Soulier syndrome and the role of the GPIb-V-IX complex in such anomalies are long-standing questions. Ultrastructural analysis of bone marrow in a limited number of patients and in a mouse model lacking the GPIbα subunit have suggested the preservation of megakaryocyte differentiation and the occurrence of defects during later stages of platelet formation in the absence of GPIb-V-IX.[4-7] The present study provides new insight into these issues following examination of various aspects of megakaryopoiesis *in situ* and culture of cells from a mouse model of GPIbβ deficiency. After demonstrating normal platelet survival, we used bone marrow analyses to rule out abnormal progenitor commitment, endoreplication or megakaryocyte maturation as causes of macrothrombocytopenia.

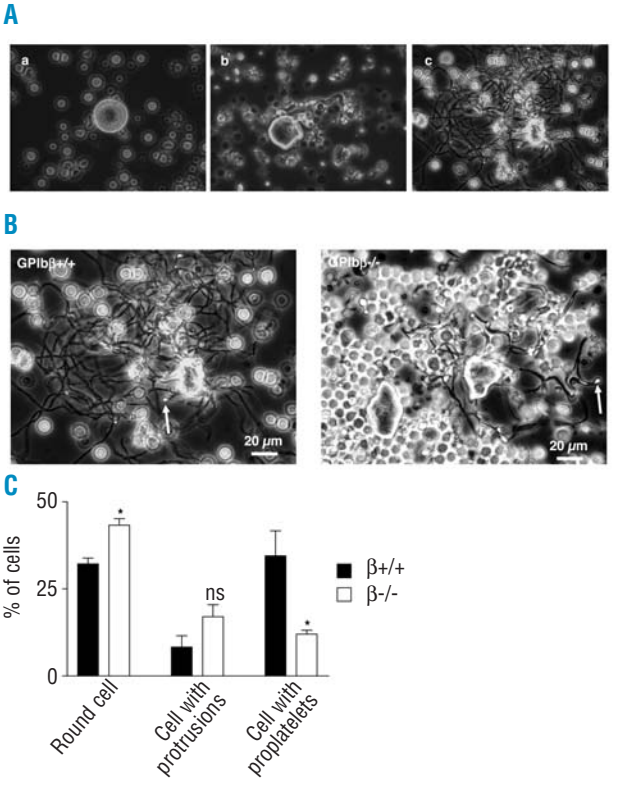

Figure 6. Abnormal proplatelet formation in bone marrow explants from GPIbβ$^{-/-}$ mice. Bone marrow sections (0.5 mm) from GPIbβ$^{+/+}$ and GPIbβ$^{-/-}$ adult mice were incubated in serum-supplemented Tyrode's buffer at 37°C and observed by time-lapse videomicroscopy. (A) Representative pictures of GPIbβ$^{+/+}$ megakaryocytes at the periphery of the bone marrow exhibiting a round immature morphology (a), a single thick protrusion (b), long fragmented pseudopodia (c). (B) Comparative photographs of GPIbβ$^{+/+}$ and GPIbβ$^{-/-}$ megakaryocytes exhibiting decreased proplatelet number and size in GPIbβ$^{-/-}$ (C) Quantification of the three representative morphologies of megakaryocytes (round cell, cell with protrusion and cell with proplatelets). The percentage of cells (±SEM) was measured in three separate experiments and represented 25-28 megakaryocytes in each strain.

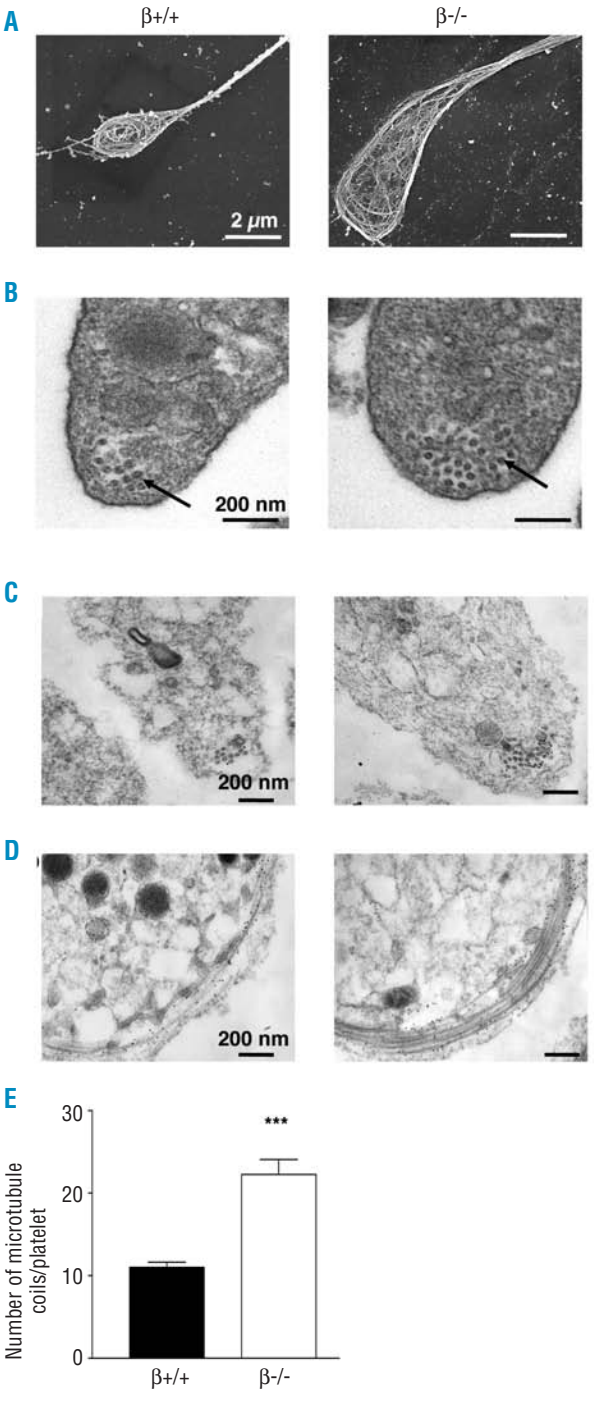

Figure 7. Proplatelets and platelets from GPIbβ$^{-/-}$ mice display an abnormal microtubular ultrastructure. (A) Scannng electron microscopy images of proplatelets after removal of the membrane by treatment with Triton X-100 detergent revealed a cytoskeleton composed of an actin meshwork with bundles of microtubules along the shafts and in the coiled elements. Increased thickness of the microtubules was observed in GPIbβ$^{-/-}$ as compared to GPIbβ$^{+/+}$ proplatelets. (B) TEM images of cultured platelets in transverse section illustrating the increased number of marginal microtubular rings in GPIbβ$^{-/-}$ as compared to GPIbβ$^{+/+}$ cells. Immunogold labeling of β-tubulin in circulating blood platelets also showed increased numbers of microtubules in the marginal band in GPIbβ$^{-/-}$ cells on transverse (C) and equatorial (D) cryosections examined by TEM. (E) Quantification of the number of microtubule coils in the marginal band on TEM images of thin sections of circulating platelets. Values are the mean±SEM for 16 individual platelets in each group.

Ultrastructural and confocal microscopic examination of bone marrow and *in vitro*-differentiated megakaryocytes identified defects in late events leading to proplatelet formation. An increased proportion of megakaryocytes differentiated in culture were unable to extend proplatelets and those that did bore fewer extensions terminated by larger coiled elements with an oversized marginal microtubular band. This combination of inefficiency in reaching the proplatelet stage and a decreased number but larger size of platelet elements would appear to be responsible for the macrothrombocytopenia in Bernard-Soulier syndrome.

The question of whether abnormal platelet survival could be a cause of thrombocytopenia in Bernard-Soulier syndrome is not settled as both decreased and normal platelet half-lives have been documented in Bernard-Soulier patients by ^{111}In-labeling.[6,33] Survival was normal in half the cases studied by Heyns *et al.*, suggesting some heterogeneity among Bernard-Soulier patients. Normal platelet survival was observed in all the GPIbβ$^{-/-}$ mice evaluated in this study, but caution should be exercised when comparing results for mice and men, especially in view of the differences in terms of platelet count and size between the two species.[34] On the other hand, the results in mice and the above previous observation of patients with a normal platelet half-life suggest that in addition to species differences, technical factors could be responsible for the shorter survival measured in some individuals. Giant platelets are difficult to isolate and might be activated during ^{111}In-labeling[33] and artificially removed from the circulation upon re-injection into patients. This difficulty could be circumvented in our mouse model as the *in vivo* biotin labeling method avoids the platelet isolation and re-injection required in isotopic techniques. Although our results cannot be generalized to humans, they do suggest that the macrothrombocytopenia observed in the absence of the GPIb-V-IX complex is essentially linked to defective thrombopoiesis.

A lack of GPIb-V-IX did not affect megakaryocyte progenitors as assessed in clonogenic assays. This is consistent with expression of GPIb-V-IX only after megakaryocyte commitment but appears to contradict the decreased number of CD34^{+} derived CFU-megakaryocytes detected by incubation with antibodies against GPIbα.[9,10,35] However, receptor occupancy and genetic inactivation results should be compared with caution, especially in view of the reported Fc-receptor activating properties of GPIbα monoclonal antibodies, which are possibly more suitable to probe mechanisms of immune-mediated thrombocytopenia.[36]

Macrothrombocytopenia was likewise not caused by an inability of progenitors to differentiate into identifiable megakaryocytes since GPIbβ$^{-/-}$ bone marrow contained an increased rather than a decreased number of these characteristic large cells. The reasons for this increase is not known, although it could be due to thrombopoietin-dependent reactive thrombopoiesis in response to low platelet counts.[37] Plasma levels of thrombopoietin were not significantly different in GPIbβ$^{+/+}$ and GPIbβ$^{-/-}$ mice (*data not shown*).

After ruling out impaired megakaryocyte commitment or differentiation in GPIbβ deficiency, we looked

for a maturation defect. A hallmark of mature megakaryocytes is their capacity to reach high ploidy levels through endomitosis.[38] An analysis of bone marrow showed a normal ploidy distribution in GPIbβ$^{-/-}$ megakaryocytes. This was somewhat unexpected since an increased proportion of high ploidy megakaryocytes has been reported in a Bernard-Soulier patient[6] and in mice expressing a GPIbα transgene deleted in its cytoplasmic domain,[20] the latter effect being observed only under stress thrombopoiesis. Our present knowledge of the mechanisms regulating endomitosis is nevertheless incomplete and the involvement of the GPIb-V-IX complex in this process remains an open question.

The most noticeable maturation defects in GPIbβ$^{-/-}$ cells concerned late steps known to be independent of endomitosis. Ultrastructural examination of the bone marrow revealed an abnormal expansion of the intracellular membrane network, the DMS, which is a characteristic of terminally differentiated megakaryocytes.[39,40] Since this defect has also been observed in GPIbα-deficient mice,[9,41] it would seem that the entire complex and not just a specific subunit is required for the formation of internal membranes. Invagination of the megakaryocyte plasma membrane was proposed to involve PI-4,5-P2 phosphatidyl inositol and local assembly of the actin network.[24] The role of the GPIb-V-IX complex in this process is still a mystery but could involve its ability to structure the submembranous actin network through its capacity to bind intracellular filamin.[18] Another possibility is that the hyperglycosylated macroglycopeptide domain of GPIbα could participate in membrane invagination. This might explain the incomplete normalization of platelet size and count in GPIbα knockout mice by a transgene lacking the entire extracellular domain, including the macroglycopeptide.[20] The reduced DMS, by limiting the membrane reservoir, probably affects the capacity to extend proplatelets. A similar reduction in the DMS was observed in megakaryocytes in a mouse model of *MYH9* deficiency resulting in decreased platelet production.[42]

In addition to defective membrane mobilization, we found signs of an abnormal distribution of the cytoskeleton. A wider peripheral zone was observed in GPIbβ$^{-/-}$ bone marrow megakaryocytes, a defect not previously documented in Bernard-Soulier syndrome. The function of this agranular region enriched in cytoskeletal proteins such as actin and myosin is still unknown. Tablin *et al.* suggested that its disorganization precedes and is required for the extension of proplatelets,[32] while others have proposed that it is required for attachment to the sinusoids.[43] A second anomaly which could be related to the cytoskeleton is the smaller degree of branching of GPIbβ$^{-/-}$ proplatelets, this branching being dependent on the recruitment of an actin-based cytoskeleton.[32] Loss of GPIbα anchorage to actin could contribute to this reorganization. The recent functional mapping and structural characterization of the GPIb-filamin complex now offers ways to test its specific involvement in platelet biogenesis.[18,44]

The most striking cytoskeletal anomaly was the doubling of the number of tubulin filaments in the marginal band of coiled proplatelet elements and individual platelets. An increased number of microtubule coils has been previously observed in giant platelets from patients with May-Hegglin or Epstein's disease[45] but to our knowledge this has never been reported in Bernard-Soulier patients. Our results in a mouse model and in patients' platelets (*Online Supplementary Figure S1*) thus provide additional evidence that this could be a general defect in giant platelet disorders. Moreover, the observation of an increase in microtubule coils in disorders with distinct origins (anomaly of a contractile protein and lack of a surface receptor, respectively) raises the possibility that this might be a reflection rather than a cause of giant platelet production. In fact, we have limited knowledge of the determinants that restrict the number of microtubule coils in normal platelets to approximately seven to eleven. Dynamic reorganization of tubulin is required for proplatelet extension and occurs through polymerization and sliding mechanisms.[25] Our results suggest that the GPIb-V-IX complex could regulate tubulin reorganization, possibly through a direct or indirect interaction. The total tubulin content influences this mechanism as deficiency of the β1 isoform produces fewer platelets containing two to three coils per cell,[46] but the effect of tubulin overexpression is unknown. Searches for tubulin-interacting proteins in megakaryocytes have not yielded clear partners and mechanisms involved in the coiling process. Recently, however, a two-hybrid screen of a mouse megakaryocyte library has revealed RanBP10, in similar distribution in the microtubular coil, which could play a role in the process of microtubule mobilization during proplatelet formation.[47] There is to date no indication of a direct or indirect link, through a partner such as Ran BP10, between GPIb and tubulin.

One unexpected finding was that both circulating and cultured GPIbβ-deficient platelets displayed the prototypical discoid shape of normal cells whereas Bernard-Soulier platelets have been classically described as spherical with irregular surfaces.[48] Our earlier analyses of Bernard-Soulier platelets were performed in citrate- or ACD-anticoagulated samples after long sedimentation times to separate large platelets from leukocytes. Under these conditions, spherical and irregular morphologies were observed. More recently, platelets were quickly fractionated on Ficoll and washed. Scanning electron micrographs of Bernard-Soulier platelets prepared by this method (*Online Supplementary Figure S2*) revealed a flat, discoid morphology, similar to that of control platelets. Quantitative analyses on more than 400 individual platelets showed an overwhelming proportion of discoid platelets in the two Bernard-Soulier patients (*Online Supplementary Figure S3*). If the question of the native shape in the circulation remains open, our data indicate that both human Bernard-Soulier and GPIbβ$^{-/-}$ mouse platelets have the capacity to adopt a discoid morphology with a typical marginal band of microtubules, despite deficiency of the GPIb-V-IX complex and lack of intracellular linking with the cytoskeleton.

Another unexpected result was the normal density and size of α-granules in GPIbβ$^{-/-}$ platelets. This contrasted with the report of α-granules of increased size in another GPIbβ$^{-/-}$ strain[49] which was attributed to up-reg-

ulation of SEPT5 expression whose gene is located 5' to the *GPIBB* gene and modulates exocytosis. This discrepancy is difficult to explain but does not appear to be due to the targeting strategy which was very similar in the two studies with insertion of a neo cassette at the same 5'-restriction site, and only differed in the length of the 3' untranslated region .

Whereas diameters of proplatelet tips (Figure 5B) are similar to those of circulating platelets in GPIbβ$^{+/+}$ animals (Figure 5D), differences are observed in GPIbβ$^{-/-}$ animals. One possibility is that only the smaller platelet buds are efficiently released in the medium or alternatively that some cytoskeletal reorganization occurs after release, leading to contraction of their size.

Our observation of a very similar abnormal proplatelet formation in bone marrow explants and in culture suspensions, in the absence of contact with immobilized cells or matrices, is a strong indication that the defects originate from within the megakaryocyte. It has been proposed that the microenvironment and cell-matrix interactions participate in megakaryocyte differentiation and proplatelet formation.[6,50] von Willebrand factor, an extracellular matrix protein and an important ligand of the GPIb-V-IX complex, could conceivably modulate platelet formation. Our present findings, together with the fact that complete deficiency of von Willebrand factor does not result in macrothrombocytopenia,[13] would however appear to rule out involvement of the GPIb/von Willebrand factor axis. In a very recent study, Balduini *et al.*[51] investigated proplatelet production of human megakaryocytes on different matrices and showed that it was prevented upon cleavage of GPIbα by the metalloproteinase mocarhagin or its blockade by an antibody. These treatments prevented proplatelet formation on von Willebrand factor as well as on fibrinogen and in cells in suspension, indicating a role of the receptor not limited to the von Willebrand factor axis possibly through other determinants such as transmembrane or intracellular domains.

In conclusion, extensive study of megakaryopoiesis in a mouse model of Bernard-Soulier syndrome identified a requirement for the GPIb-V-IX complex in the critical stage of proplatelet formation. This was revealed by abnormalities in the recruitment of cytoplasmic membranes and dynamic reorganization of the tubulin cytoskeleton. A very recent article described similar abnormalities in proplatelet formation in megakaryocytes differentiated from individuals heterozygous for the Bernard-Soulier syndrome Bolzano mutation.[52] These results provide a good indication that the mouse model properly reproduces the defects in the human disease. Therefore, available GPIbβ- and by extension GPIbα-deficient mice[27,49,53] represent appropriate models to pursue studies of the role of GPIb-V-IX in thrombopoiesis. Use of such models in rescue studies with selected mutagenesis of the receptor should increase our knowledge of the mechanisms of megakaryocyte maturation and platelet formation.

Authorship and Disclosures

FL and CS designed the research, CS performed the research, AE performed and analyzed electron microscopy images, CP assisted CS in all experiments, MF contributed vital tools, CS, CL, JPC, CG and FL analyzed the data and CS, AE, CL, CG and FL wrote the paper.

The authors reported no potential conflicts of interest.

References

1. Bernard J, Soulier JP. [Not Available.]. Sem Hop 1948;24:3217-23.
2. Nurden AT, Didry D, Rosa JP. Molecular defects of platelets in Bernard-Soulier syndrome. Blood Cells 1983;9:333-58.
3. Berndt MC, Du XP, Booth WJ. Ristocetin-dependent reconstitution of binding of von Willebrand factor to purified human platelet membrane glycoprotein Ib-IX complex. Biochemistry 1988;27:633-40.
4. Italiano JE Jr, Shivdasani RA. Megakaryocytes and beyond: the birth of platelets. J Thromb Haemost 2003;1:1174-82.
5. Schulze H, Shivdasani RA. Mechanisms of thrombopoiesis. J Thromb Haemost 2005;3:1717-24.
6. Tomer A, Scharf RE, McMillan R, Ruggeri ZM, Harker LA. Bernard-Soulier syndrome: quantitative characterization of megakaryocytes and platelets by flow cytometric and platelet kinetic measurements. Eur J Haematol 1994;52:193-200.
7. Hourdille P, Benabdallah S, Belloc F, Nurden AT. Distribution of glycoprotein IIb-IIIa complexes in the surface membranes of human platelets and megakaryocytes. Br J Haematol 1985;59:171-82.
8. Nurden P, Nurden A. Giant platelets, megakaryocytes and the expression of glycoprotein Ib-IX complexes. C R Acad Sci III 1996;319:717-26.
9. Poujol C, Ware J, Nieswandt B, Nurden AT, Nurden P. Absence of GPIbα is responsible for aberrant membrane development during megakaryocyte maturation: ultrastructural study using a transgenic model. Exp Hematol 2002;30:352-60.
10. Lepage A, Leboeuf M, Cazenave JP, de la Salle C, Lanza F, Uzan G. The α(IIb)β(3) integrin and GPIb-V-IX complex identify distinct stages in the maturation of CD34(+) cord blood cells to megakaryocytes. Blood 2000;96:4169-77.
11. Debili N, Kieffer N, Nakazawa M, Guichard J, Titeux M, Cramer E, et al. Expression of platelet glycoprotein Ib by cultured human megakaryocytes: ultrastructural localization and biosynthesis. Blood 1990;76:368-76.
12. Lopez JA, Andrews RK, Afshar-Kharghan V, Berndt MC. Bernard-Soulier syndrome. Blood 1998;91:4397-418.
13. Denis C, Methia N, Frenette PS, Rayburn H, Ullman-Culleré M, Hynes RO, Wagner DD. A mouse model of severe von Willebrand disease: defects in hemostasis and thrombosis. Proc Natl Acad Sci USA 1998;95:9524-9.
14. Subramaniam M, Frenette PS, Saffaripour S, Johnson RC, Hynes RO, Wagner DD. Defects in hemostasis in P-selectin-deficient mice. Blood 1996;87:1238-42.
15. Nurden P, Debili N, Vainchenker W, Bobe R, Bredoux R, Corvazier E, et al. Impaired megakaryocytopoiesis in type 2B von Willebrand disease with severe thrombocytopenia. Blood 2006;108:2587-95.
16. Takahashi R, Sekine N, Nakatake T. Influence of monoclonal antiplatelet glycoprotein antibodies on in vitro human megakaryocyte colony formation and proplatelet formation. Blood 1999;93:1951-8.
17. Feng S, Lu X, Kroll MH. Filamin A binding stabilizes nascent glycoprotein Ibalpha trafficking and thereby enhances its surface expression. J Biol Chem 2005;280:6709-15.

18. Hartwig JH, Italiano JE Jr. Cytoskeletal mechanisms for platelet production. Blood Cells Mol Dis 2006;36:99-103.
19. Rojnuckarin P, Kaushansky K. Actin reorganization and proplatelet formation in murine megakaryocytes: the role of protein kinase c alpha. Blood 2001;97:154-61.
20. Kanaji T, Russell S, Cunningham J, Izuhara K, Fox JE, Ware J. Megakaryocyte proliferation and ploidy regulated by the cytoplasmic tail of glycoprotein Ibalpha. Blood 2004;104:3161-8.
21. Lecine P, Villeval JL, Vyas P, Swencki B, Xu Y, Shivdasani RA. Mice lacking transcription factor NF-E2 provide in vivo validation of the proplatelet model of thrombocytopoiesis and show a platelet production defect that is intrinsic to megakaryocytes. Blood 1998;92:1608-16.
22. Hartwig J, Italiano J Jr. The birth of the platelet. J Thromb Haemost 2003;1:1580-6.
23. Italiano JE Jr, Patel-Hett S, Hartwig JH. Mechanics of proplatelet elaboration. J Thromb Haemost 2007;5 (Suppl 1):18-23.
24. Schulze H, Korpal M, Hurov J, Kim SW, Zhang J, Cantley LC, et al. Characterization of the megakaryocyte demarcation membrane system and its role in thrombopoiesis. Blood 2006;107:3868-75.
25. Italiano JE Jr, Lecine P, Shivdasani RA, Hartwig JH. Blood platelets are assembled principally at the ends of proplatelet processes produced by differentiated megakaryocytes. J Cell Biol 1999;147:1299-312.
26. Patel-Hett S, Richardson JL, Schulze H, Drabek K, Isaac NA, Hoffmeister K, et al. Visualization of microtubule growth in living platelets reveals a dynamic marginal band with multiple microtubules. Blood 2008;111: 4605-16.
27. Strassel C, Nonne C, Eckly A, David T, Leon C, Freund M, et al. Decreased thrombotic tendency in mouse models of the Bernard-Soulier syndrome. Arterioscler Thromb Vasc Biol 2007;27:241-7.
28. Peng J, Friese P, Heilmann E, George JN, Burstein SA, Dale GL. Aged platelets have an impaired response to thrombin as quantitated by P-selectin expression. Blood 1994;83: 161-6.
29. Hartwig JH, DeSisto M. The cytoskeleton of the resting human blood platelet: structure of the membrane skeleton and its attachment to actin filaments. J Cell Biol 1991;112:407-25.
30. Cazenave JP, Ohlmann P, Cassel D, Eckly A, Hechler B, Gachet C. Preparation of washed platelet suspensions from human and rodent blood. Methods Mol Biol 2004;272: 13-28.
31. Zucker-Franklin D. Megakaryocytes and platelets. In: Zucker-Franklin D, Grossi CE, eds. Atlas of Blood Cells. Vol. 2 (ed Edi-Ermes). Milan;2003: 788-91.
32. Tablin F, Castro M, Leven RM. Blood platelet formation in vitro. The role of the cytoskeleton in megakaryocyte fragmentation. J Cell Sci 1990;97(Pt 1):59-70.
33. Heyns Adu P, Badenhorst PN, Wessels P, Pieters H, Lotter MG. Kinetics, in vivo redistribution and sites of sequestration of indium-111-labelled platelets in giant platelet syndromes. Br J Haematol 1985;60: 323-30.
34. Tsakiris DA, Scudder L, Hodivala-Dilke K, Hynes RO, Coller BS. Hemostasis in the mouse (Mus musculus): a review. Thromb Haemost 1999;81:177-88.
35. Vainchenker W, Kieffer N. Human megakaryocytopoiesis: in vitro regulation and characterization of megakaryocytic precursor cells by differentiation markers. Blood Rev 1988;2:102-7.
36. Nieswandt B, Bergmeier W, Rackebrandt K, Gessner JE, Zirngibl H. Identification of critical antigen-specific mechanisms in the development of immune thrombocytopenic purpura in mice. Blood 2000;96: 2520-7.
37. Kaushansky K. Thrombopoietin and the hematopoietic stem cell. Ann N Y Acad Sci 2005;1044:139-41.
38. Battinelli EM, Hartwig JH, Italiano JE Jr. Delivering new insight into the biology of megakaryopoiesis and thrombopoiesis. Curr Opin Hematol 2007;14:419-26.
39. Cramer EM. Megakaryocyte structure and function. Curr Opin Hematol 1999;6:354-61.
40. Zucker-Franklin D. Megakaryocyte and platelet structure in thrombocytopoiesis: the effect of cytokines. Stem Cells 1996;14(Suppl 1):1-17.
41. Ware J, Russell S, Ruggeri ZM. Generation and rescue of a murine model of platelet dysfunction: the Bernard-Soulier syndrome. Proc Natl Acad Sci USA 2000;97:2803-8.
42. Eckly A, Strassel C, Freund M, Cazenave JP, Lanza F, Gachet C, Leon C. Abnormal megakaryocyte morphology and proplatelet formation in mice with megakaryocyte-restricted MYH9 inactivation. Blood 2009;113:3182-9.
43. Thiele J, Galle R, Sander C, Fischer R. Interactions between megakaryocytes and sinus wall. An ultrastructural study on bone marrow tissue in primary (essential) thrombocythemia. J Submicrosc Cytol Pathol 1991;23:595-603.
44. Williamson D, Pikovski I, Cranmer SL, Mangin P, Mistry N, Domagala T, et al. Interaction between platelet glycoprotein Ibalpha and filamin-1 is essential for glycoprotein Ib/IX receptor anchorage at high shear. J Biol Chem 2002;277:2151-9.
45. White JG, Sauk JJ. The organization of microtubules and microtubule coils in giant platelet disorders. Am J Pathol 1984;116:514-22.
46. Schwer HD, Lecine P, Tiwari S, Italiano JE Jr, Hartwig JH, Shivdasani RA. A lineage-restricted and divergent beta-tubulin isoform is essential for the biogenesis, structure and function of blood platelets. Curr Biol 2001;11:579-86.
47. Schulze H, Dose M, Korpal M, Meyer I, Italiano JE Jr, Shivdasani RA. RanBP10 is a cytoplasmic guanine nucleotide exchange factor that modulates noncentrosomal microtubules. J Biol Chem 2008;283: 14109-19.
48. Nurden P, Nurden AT. Congenital disorders associated with platelet dysfunctions. Thromb Haemost 2008;99:253-63.
49. Kato K, Martinez C, Russell S, Nurden P, Nurden A, Fiering S, Ware J. Genetic deletion of mouse platelet glycoprotein Ibbeta produces a Bernard-Soulier phenotype with increased alpha-granule size. Blood 2004;104:2339-44.
50. Sabri S, Jandrot-Perrus M, Bertoglio J, Farndale RW, Mas VM, Debili N, et al. Differential regulation of actin stress fiber assembly and proplatelet formation by $\alpha 2\beta 1$ integrin and GPVI in human megakaryocytes. Blood 2004;104:3117-25.
51. Balduini A, Pallotta I, Malara A, Lova P, Pecci A, Viarengo G, et al. Adhesive receptors, extracellular proteins and myosin IIA orchestrate proplatelet formation by human megakaryocytes. J Thromb Haemost 2008;6:1900-7.
52. Balduini A, Malara A, Pecci A, Badalucco S, Bozzi V, Pallotta I, et al. Proplatelet formation in heterozygous Bernard-Soulier syndrome type Bolzano. J Thromb Haemost 2009;7: 478-84.
53. Kanaji T, Russell S, Ware J. Amelioration of the macrothrombocytopenia associated with the murine Bernard-Soulier syndrome. Blood 2002;100:2102-7.